UCLA
UCLA Previously Published Works

Title

A neurodevelopmental disorder associated with an activating de novo missense variant in ARF1.

Permalink

https://escholarship.org/uc/item/751023hq

Journal

Human Molecular Genetics, 32(7)

Authors

Ishida, Morié
Otero, María
Freeman, Christina
et al.

Publication Date

2023-03-20

DOI

10.1093/hmg/ddac279

Peer reviewed

A neurodevelopmental disorder associated with an activating *de novo* missense variant in *ARF1*

Morié Ishida[1], María G. Otero[2], Christina Freeman[2], Pedro A. Sánchez-Lara[3], Carlos M. Guardia[1,4], Tyler Mark. Pierson ![ORCID][2,5,6,7,*] and Juan S. Bonifacino[1,*]

[1]Neurosciences and Cellular and Structural Biology Division, Eunice Kennedy Shiver National Institute of Child Health and Human Development, National Institutes of Health, Bethesda, MD 20892, USA
[2]Board of Governors Regenerative Medicine Institute, Cedars-Sinai Medical Center, Los Angeles, CA 90048, USA
[3]Division of Medical Genetics, Department of Pediatrics, Cedars-Sinai Medical Center, Los Angeles, CA 90048, USA
[4]Reproductive and Developmental Biology Laboratory, National Institute of Environmental Health Sciences, National Institutes of Health, Research Triangle Park, NC 27703, USA
[5]Division of Pediatric Neurology, Department of Pediatrics, Cedars-Sinai Medical Center, Los Angeles, CA 90048, USA
[6]Department of Neurology, Cedars-Sinai Medical Center, Los Angeles, CA 90048, USA
[7]Center for the Undiagnosed Patient, Cedars-Sinai Medical Center, Los Angeles, CA 90048, USA

*To whom correspondence should be addressed: Tyler Mark Pierson, Tel: +1 3102488558; Fax: +1 3102488066; Email: tyler.pierson@cshs.org. Juan Bonifacino, Tel: +1 3014966368; Fax: +1 3014029319; Email: juan.bonifacino@nih.gov

Abstract

ADP-ribosylation factor 1 (ARF1) is a small GTPase that regulates membrane traffic at the Golgi apparatus and endosomes through recruitment of several coat proteins and lipid-modifying enzymes. Here, we report a pediatric patient with an *ARF1*-related disorder because of a monoallelic *de novo* missense variant (c.296 G > A; p.R99H) in the *ARF1* gene, associated with developmental delay, hypotonia, intellectual disability and motor stereotypies. Neuroimaging revealed a hypoplastic corpus callosum and subcortical white matter abnormalities. Notably, this patient did not exhibit periventricular heterotopias previously observed in other patients with *ARF1* variants (including p.R99H). Functional analysis of the R99H-ARF1 variant protein revealed that it was expressed at normal levels and properly localized to the Golgi apparatus; however, the expression of this variant caused swelling of the Golgi apparatus, increased the recruitment of coat proteins such as coat protein complex I, adaptor protein complex 1 and GGA3 and altered the morphology of recycling endosomes. In addition, we observed that the expression of R99H-ARF1 prevented dispersal of the Golgi apparatus by the ARF1-inhibitor brefeldin A. Finally, protein interaction analyses showed that R99H-ARF1 bound more tightly to the ARF1-effector GGA3 relative to wild-type ARF1. These properties were similar to those of the well-characterized constitutively active Q71L-ARF1 mutant, indicating that the pathogenetic mechanism of the R99H-ARF1 variant involves constitutive activation with resultant Golgi and endosomal alterations. The absence of periventricular nodular heterotopias in this R99H-ARF1 subject also indicates that this finding may not be a consistent phenotypic expression of all *ARF1*-related disorders.

Introduction

ADP-ribosylation factors (ARFs) constitute a family of small GTPases that consists of five different proteins in humans (ADP-ribosylation factor 1 (ARF1) and ARF3–ARF6) (1,2). Based on amino acid sequence homology, the five human ARFs have been grouped into three classes: class I (ARF1 and ARF3, 96% identity to each other), class II (ARF4 and ARF5, 90% identity to each other, and 82% identity to ARF1) and class III (ARF6, 68% identity to ARF1). Both class I and II ARFs are mainly localized to the Golgi apparatus, where they regulate the structure and function of this organelle. In contrast, the class III ARF6 localizes to the plasma membrane and regulates the cortical actin cytoskeleton and endosomal membrane recycling. Among the Golgi-localized ARFs, ARF1 is the most abundant (3) and most widely studied (1,2).

Like other small GTPases, ARF1 can switch between active GTP-bound and inactive GDP-bound conformations (1,2). GTP-bound ARF1 associates with membranes via an N-terminal myristoylated, amphipathic α-helix, and binds multiple effectors including coat proteins and lipid-modifying enzymes, via its switch 1 and 2 regions (shown in blue and red in Fig. 1A and B). On the other

hand, GDP-bound ARF1 is cytosolic and is unable to bind these effectors. The exchange of GDP by GTP on ARF1 is mediated by guanine nucleotide exchange factors (GEFs), whereas the hydrolysis of GTP to GDP is mediated by GTPase-activating proteins (1,2). The fungal metabolite brefeldin A (BFA) inhibits ARF1 function by stabilizing the formation of a complex between ARF1-GDP and some ARF1 GEFs (4). Of note, substitution of residue Q71 with leucine (Q71L) locks ARF1 into its GTP-bound conformation (5–7) (Fig. 1A and B), whereas substitution of residue T31 with asparagine (T31N) locks ARF1 into its GDP-bound conformation (5). As a consequence, these mutants behave as constitutively active or dominant-negative proteins, respectively, when expressed in cells.

Among the best characterized ARF1 effectors are coat proteins that regulate anterograde and/or retrograde transport at the Golgi apparatus and the *trans*-Golgi network (TGN) (1,2). ARF1-regulated coat proteins include coat protein complex I (COPI) (9,10), adaptor protein (AP) complex 1 (AP-1) (11), AP-3 (12), AP-4 (13) and the Golgi-localized, γ-ear-containing, ADP-ribosylation factor-binding proteins (GGAs) (GGA1–GGA3) (14,15). ARF1
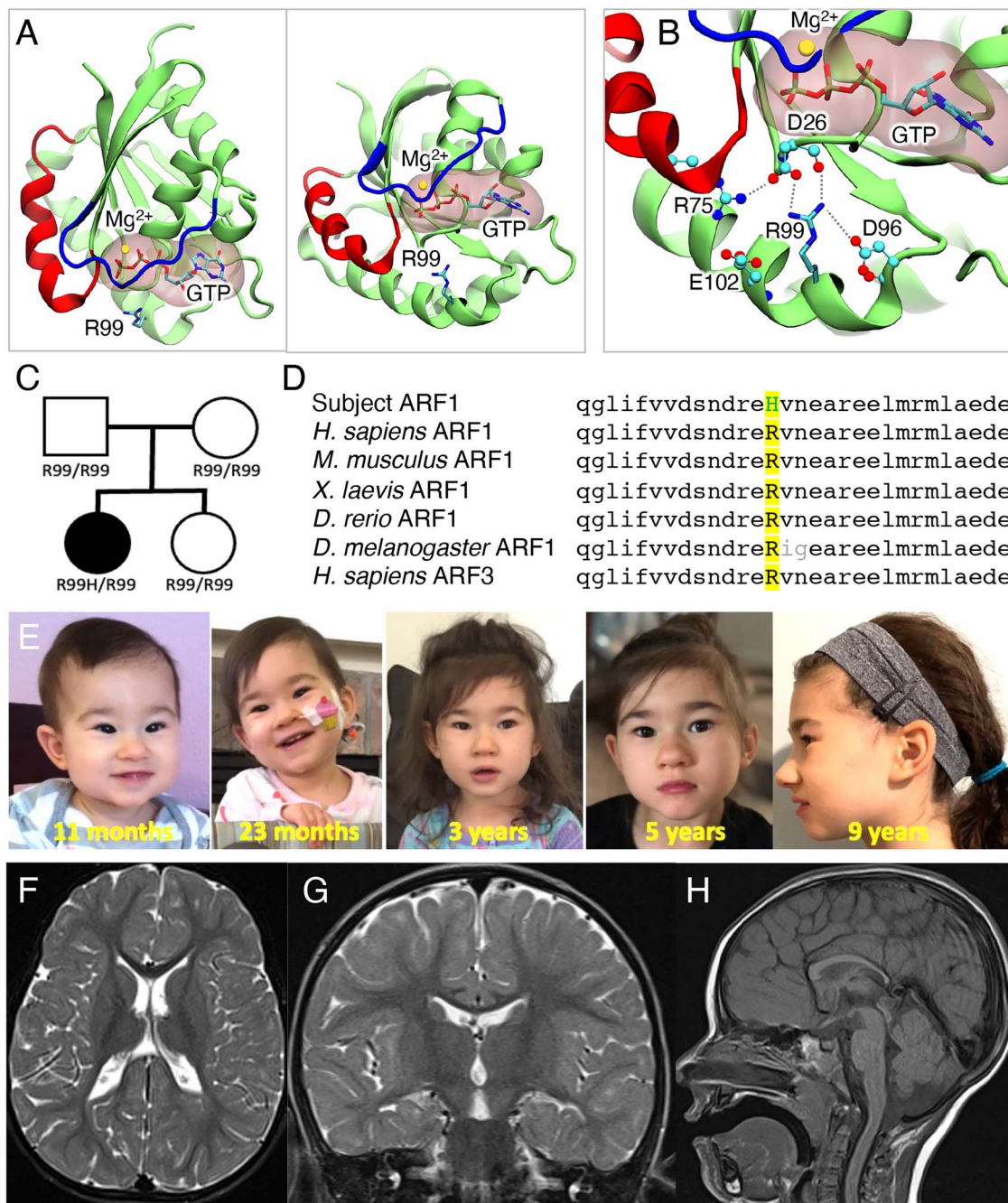
Figure 1. Location of R99 and clinical features of the subject. (**A**) Crystal structure of mouse ARF1-GTP (amino acids 16–181) (PDBID: 1O3Y) (the amino-acid sequences of mouse and human ARF1 are identical) highlighting R99, GTP in stick representation, Mg^{2+} in yellow, switch 1 (amino acids 42–52) in blue, and switch 2 (amino acids 70–85) in red. The surface of GTP-Mg^{2+} is shown in pink to highlight the GTP-binding site. (**B**) Close-up of the ARF1-GTP structure showing the relationship of R99 to neighboring residues (at <4 Å, except for E102, which is at 4.5 Å). R99 interacts with D26, a residue that may influence stabilization of water for hydrolysis of GTP, as previously proposed for ARF3 (8). Substitution of histidine for R99 would perturb this stabilization, reducing GTP hydrolysis and thus resulting in a gain-of-function phenotype. (**C**) Family pedigree. (**D**) Amino-acid sequence of the subject's R99H variant and conservation of the R99 residue in ARF1 across vertebrate and invertebrate species. The sequences of human ARF1 and ARF3 in this region are identical. (**E**) Facial appearance of the child from infancy through 9 years. (**F–H**) Brain MRI at 3 years [(F) axial T2, (G) coronal T2 and (H) sagittal T1 sequences] showed a hypoplastic, but fully developed corpus callosum along with nonspecific T2-hyperintensities within the subcortical white matter that were most pronounced along the medial parietal convexities. PVNH or other heterotopias were not present.

functions to recruit all of these coat proteins to membranes, promoting the formation of transport carriers and the capture of specific cargos into the carriers (16,17). Each of these coat proteins mediates a specific transport process. For example, COPI mediates retrograde transport between Golgi cisternae, and from the *cis*-Golgi to the endoplasmic reticulum (ER). AP-1 mediates bidirectional transport between the TGN and endosomes and is

particularly important for cargo sorting to the basolateral surface of epithelial cells and the somatodendritic domain of neurons. AP-3 mediates sorting to lysosome-related organelles such as melanosomes and platelet dense bodies, whereas AP-4 is involved in export of select cargos such as the autophagy protein ATG9A from the TGN. Finally, the GGAs sort cargos such as mannose 6-phosphate receptors from the TGN to endosomes (16,17).

ARF1 and some of these coat proteins have also been shown to localize to endosomes, where they play additional roles in transport. Treatment of cells with BFA causes dissociation of these coat proteins from membranes, which blocks their respective transport steps (14,15,18–22). In the case of the Golgi apparatus, BFA treatment leads to dispersal and redistribution of resident Golgi proteins to ER-exit sites (23,24).

Although the cellular functions of ARF1 have been extensively studied, its physiological roles in whole organisms are less well understood. This is in part because of the early embryonic lethality of *Arf1*-null mice (25). Recent studies in a small number of human subjects with *de novo* mutations in *ARF1* indicated that ARF1 plays a particularly critical role in the development of the central nervous system (CNS). A previous report identified three unrelated subjects with *de novo* monoallelic missense *ARF1* variants using a missense-depletion method for variant detection (8). This ARF1-related disorder was termed periventricular nodular heterotopia (PVNH) type 8 (MIM#618185), a condition in which neurons fail to completely migrate from the ventricular zone to the cortex during development (although it is unclear if all the reported subjects had evidence of heterotopias). The proband was a 9-year-old male with a missense variant (c.103 T > C; p.Y35H) who presented with developmental delays (DD), attention-deficit/hyperactivity disorder and intellectual disability (ID) associated with diminished white matter on brain magnetic resonance imaging (MRI). He was a former full-term child with normal growth parameters and had never had a seizure. The second subject was a 15-year-old female with a different missense variant (c.379 A > G; p.K127E) associated with DD, ID, spasticity, epilepsy and language regression. Her brain MRI was reported as having a 'delay in myelination', cortical thinning and vermian atrophy. The third patient possessed a missense variant (c.296 G > A; p.R99H), but had limited clinical information presented (sex and age were also unreported). This subject was noted to have seizures associated with abnormal neuroimaging that consisted of periventricular heterotopias and delayed myelination in childhood. Subsequent imaging over 10 years later also showed significant cerebral underdevelopment. The p.K127E variant was also reported in two other subjects with neurodevelopmental disorders, but these were not extensively characterized (26,27).

These missense substitutions were located within functional regions of ARF1 that may affect GDP/GTP binding or GTP hydrolysis. The Y35H variant is located near the nucleotide-binding site and was expressed at similar levels than the wild-type (WT) protein when transfected into HEK293T cells, although it had decreased nucleotide activation in this context (8). The K127E variant also involves the nucleotide-binding site and was previously reported to be important for ARF1 function in both yeast and Entamoeba model systems (28,29). Finally, the R99H variant involves a residue that appears to be in direct contact with at least one nucleotide-binding residue (D26, Fig. 1A and B), but no functional analysis had been performed until the current study.

Here, we report a 9-year-old female patient with a *de novo* monoallelic missense variant (c.296 G > A; p.R99H) in *ARF1* associated with DD, ID, hypotonia, feeding issues, failure-to-thrive, strabismus and motor stereotypies. Neuroimaging showed a hypoplastic corpus callosum combined with subcortical white matter abnormalities, without periventricular heterotopias. Functional analysis of the R99H-ARF1 protein revealed that it was expressed at normal levels and properly localized to the Golgi apparatus; however, the expression of this variant caused swelling of the Golgi apparatus, increased the recruitment of coat proteins to the Golgi apparatus and altered the morphology of recycling endosomes. Moreover, effector-binding assays showed that R99H-ARF1 bound more tightly to GGA3 relative to WT-ARF1. Finally, the expression of R99H-ARF1 prevented dispersal of the Golgi apparatus by BFA. These properties were similar to those seen with the constitutively active Q71L-ARF1 mutant, indicating that the pathogenetic mechanism of the R99H-ARF1 variant involves constitutive activation with resultant Golgi and endosomal dysfunction.

Results

Patient genotype and phenotype information

Our subject is a 9-year-old female who presented to the Cedars-Sinai Neurogenetics Clinic and Center for the Undiagnosed Patient ~3 years after exome sequencing analysis revealed a monoallelic *de novo* ARF1 variant (c.296 G > A; p.R99H) not present in her parents and her other sibling (Fig. 1C). The R99 residue in ARF1 is conserved across vertebrate and invertebrate species (Fig. 1D). The R99H variant had been reported in subject 3 noted in the Introduction (8), but was not previously observed in ~6500 subjects of European/African descent in the NHLBI Exome Sequencing Project. In the crystal structure of ARF1-GTP (30), R99 interacts with D26, a residue that is part of a phosphate-binding loop near the nucleotide-binding site (31) (Fig. 1A and B) and that could participate in GTP hydrolysis, as previously proposed for ARF3 (32).

The child's birth history had her born at 37.5 weeks of gestation to non-consanguineous parents. Her 30-year-old mother was of English–German descent and her 32-year-old father was of Japanese–Italian descent. There was no family history of neurodevelopmental or neurological disease. The pregnancy was without complications and fetal movements were normal. Her growth parameters at birth were on the lower end of normal [weight: 4th percentile (2.5 kg); length: 5th percentile (46 cm); head circumference: 6th percentile (32 cm)]. She did not feed or sleep well in the neonatal period and was described as having 'moderate' hypotonia ('not floppy'). She had difficulty gaining weight from 8 to 12 months of age and was diagnosed with failure to thrive. At 18 months, a nasogastric tube was placed and remained until 32 months of age when she reached the 15th percentile for weight. She was noted to have delayed oral motor skills and was also prescribed cyproheptadine as an appetite stimulant.

She sat up at 10 months and started walking just before her third birthday. Significant ankle pronation required supramalleolar orthoses (SMOs) to stabilize her gait. At 3 years, she did not have a pincer grasp and had poor fine motor skills. She was eating mostly pureed foods and would not drink from a cup or a bottle. She had motor stereotypies including hand wringing and rotation of her hands around her mouth (usually associated with excitement or concentration). She was nonverbal, but was making cooing sounds. Her receptive language was further advanced and she could follow one- or two-step commands. Prior to 2 years, she was diagnosed with strabismus and treated with glasses.

At 9 years, she was walking (still using SMOs) and could climb stairs and broad jump, but was not running. Fine motor skills had improved, although she could not hold a crayon well and was not writing. She could feed herself with difficulty and drooled often. Motor stereotypies were still present. She continued to be nonverbal with cooing sounds and could still only follow one- or

two-step commands. She was described as a 'happy and social' child.

As an infant/toddler she had pronounced periorbital features, which softened as she aged. She had a medial flair to her eyebrows, up-slanted palpebral fissures, deep set eyes with upper lid hooding and elongated lateral canthi accentuated by lateral lower lid fullness. She had full cheeks down to her jaw line and defined mental protuberance since infancy. She had a thin upper lip and smooth philtrum when smiling, but her philtrum appeared normal in repose (Fig. 1E).

Brain MRI at 3 years showed a hypoplastic, but fully developed corpus callosum along with nonspecific T2/FLAIR hyperintensities within the subcortical white matter that were most pronounced along the medial parietal convexities. There were no periventricular or other heterotopias (Fig. 1F–H). Electroencephalogram (EEG) at 21 months was normal, although a repeat EEG at 6 years had bilateral centrotemporal spikes (right greater than left). She has never had a witnessed seizure and was not started on anti-seizure medications.

R99H-ARF1 is expressed at normal levels but causes swelling of the Golgi apparatus

To analyze the properties of the R99H-ARF1 variant, we introduced R99H, Q71L or T31N mutations in human ARF1 tagged at the C-terminus with the HA epitope (ARF1-HA). The Q71L and T31N mutants were used as controls because of their being constitutively active, GTP-bound, and constitutively inactive, GDP-bound (or nucleotide-free), respectively (5–7). Immunoblot analysis of HEK293T cells transfected with plasmids encoding these constructs revealed similar levels of the WT, Q71L, T31N and R99H forms, indicating that none of the mutations affected the expression or stability of ARF1 (Fig. 2A and B).

Next, we performed immunofluorescence microscopy to examine the intracellular localization of the different ARF1-HA mutants and their effect on the structure of the Golgi apparatus (Fig. 2C). We observed that WT-ARF1-HA localized to the Golgi apparatus, as detected by co-staining for the Golgi marker Golgi matrix protein 130 (GM130) (Fig. 2C). The constitutively active Q71L mutant also localized to the Golgi apparatus, but caused swelling of this organelle (Fig. 2C), as previously reported (7). In contrast, the constitutively inactive T31N mutant was cytosolic and caused fragmentation of the Golgi apparatus (Fig. 2C), also in agreement with previous findings (5). Interestingly, the R99H mutant was associated with the Golgi apparatus and caused Golgi swelling comparable to that of the Q71L mutant (Fig. 2C). These observations demonstrated that the R99H mutation does not affect the recruitment of ARF1 to the Golgi apparatus, but causes swelling of this organelle comparable to that of the constitutively active Q71L mutant.

Increased activity of R99H-ARF1 in the recruitment of coat proteins to the Golgi apparatus

To further investigate the effect of the R99H mutation on ARF1 function, we examined the activity of this mutant in the recruitment of several coat proteins to the Golgi apparatus. The tested coat proteins included COPI (9,10), AP-1 (11,33) and GGA3 (14,15,34), all of which were previously shown to associate with the Golgi apparatus in an ARF-dependent manner. To carry out these experiments, we used CRISPR-Cas9 in HeLa cells to knock out (KO) *ARF1* and the closely related *ARF3* genes (ARF1–3 KO cells). We confirmed that ARF1–3 KO cells lacked the expression of both ARF1 and ARF3 (Fig. 3A). As controls, we showed that the class

II ARF4 and ARF5 were not decreased by the ARF1–3 double-KO (DKO) (Fig. 3A). In line with previous findings (9–11,14,15,33,34), we observed that ARF1–3-KO cells had greatly decreased Golgi staining for several ARF-dependent coat proteins, including the β-COP subunit of COPI, the γ1-adaptin subunit of AP-1 and the monomeric GGA3 (Fig. 3B). As expected, the expression of WT-ARF1-HA in ARF1–3 KO cells rescued the association of COPI, AP-1 and GGA3 with the Golgi apparatus (Fig. 4A–C), and the expression of Q71L-ARF1-HA rescued even more (Fig. 4A–C). Importantly, R99H-ARF1-HA showed greater rescue, comparable to that of Q71L-ARF1-HA (Fig. 4A–C). These experiments further indicated that the R99H variant is not just active, but hyperactive relative to WT ARF1.

R99H-ARF1 alters the morphology of recycling endosomes

ARF1 has also been implicated in the maintenance of recycling endosome morphology, as demonstrated by the tubulation of recycling endosomes containing the transferrin receptor (TfR) in cells treated with BFA or depleted of ARF1 and ARF3 (35–40). In agreement with these findings, we observed that ARF1–3 KO cells exhibited tubulation of TfR-containing recycling endosomes (Fig. 3B and C). The expression of WT-ARF1-HA in ARF1–3 KO cells restored the normal morphology of the recycling endosomes, whereas the expression of T31N-ARF1-HA did not (Fig. 5A). Importantly, both Q71L and R99H not only reversed tubulation, but also caused swelling of the recycling endosomal compartment (Fig. 5A). Similar experiments using WT HeLa cells showed that T31N-ARF1-HA caused tubulation, and Q71L- and R99H-ARF1-HA caused swelling of the recycling endosomal compartment (Fig. 5B). From these experiments, we concluded that the R99H-ARF1 mutant behaves similarly to the constitutively active Q71L-ARF1 mutant in the regulation of recycling endosome morphology.

R99H-ARF1 shows increased binding to GGA3 and protects the Golgi apparatus from dispersal by BFA

To directly examine if R99H-ARF1 increases the activity of ARF1, we used an effector-binding assay based on previous work from our laboratory (15). This assay consisted of a yeast two-hybrid system, in which proteins containing (i) the Gal4 DNA-binding domain (BD) fused to various ARF1-variants lacking the N-terminal myristoylated α-helix (Δ17ARF1) were co-expressed with proteins containing (ii) the VHS-GAT domains of GGA3 (GGA3-VHS-GAT) fused to the Gal4 transcriptional activation domain (AD). Interaction of any given BD-fused ARF1 mutant with AD-fused GGA3-VHS-GAT allowed for growth of yeast on medium lacking histidine and containing 3-amino-1,2,4-triazole (3AT), whereas lack of interaction was manifested as failure to grow on this medium. Using this assay, we observed that both WT- and T31N-Δ17ARF1 did not appreciably interact with GGA3-VHS-GAT, whereas both Q71L- and R99H-Δ17ARF1 displayed robust interactions, consistent with hyperactivation (Fig. 6A).

Finally, we examined the effect of R99H-ARF1-HA expression on the dispersal of the Golgi apparatus caused by BFA. In accordance with previous work (23,41,42), treatment of WT HeLa cells for 5 min with 5 μg/ml BFA dissociated COPI into the cytosol and dispersed GM130 throughout the cytoplasm (Fig. 6B). The expression of WT-ARF1-HA did not prevent Golgi dispersal by BFA (Fig. 6C and D). In contrast, the expression of Q71L- or R99H-ARF1-HA protected the Golgi apparatus from BFA-induced dispersal (Fig. 6C and D), as was previously shown for Q71L-ARF1 (7).
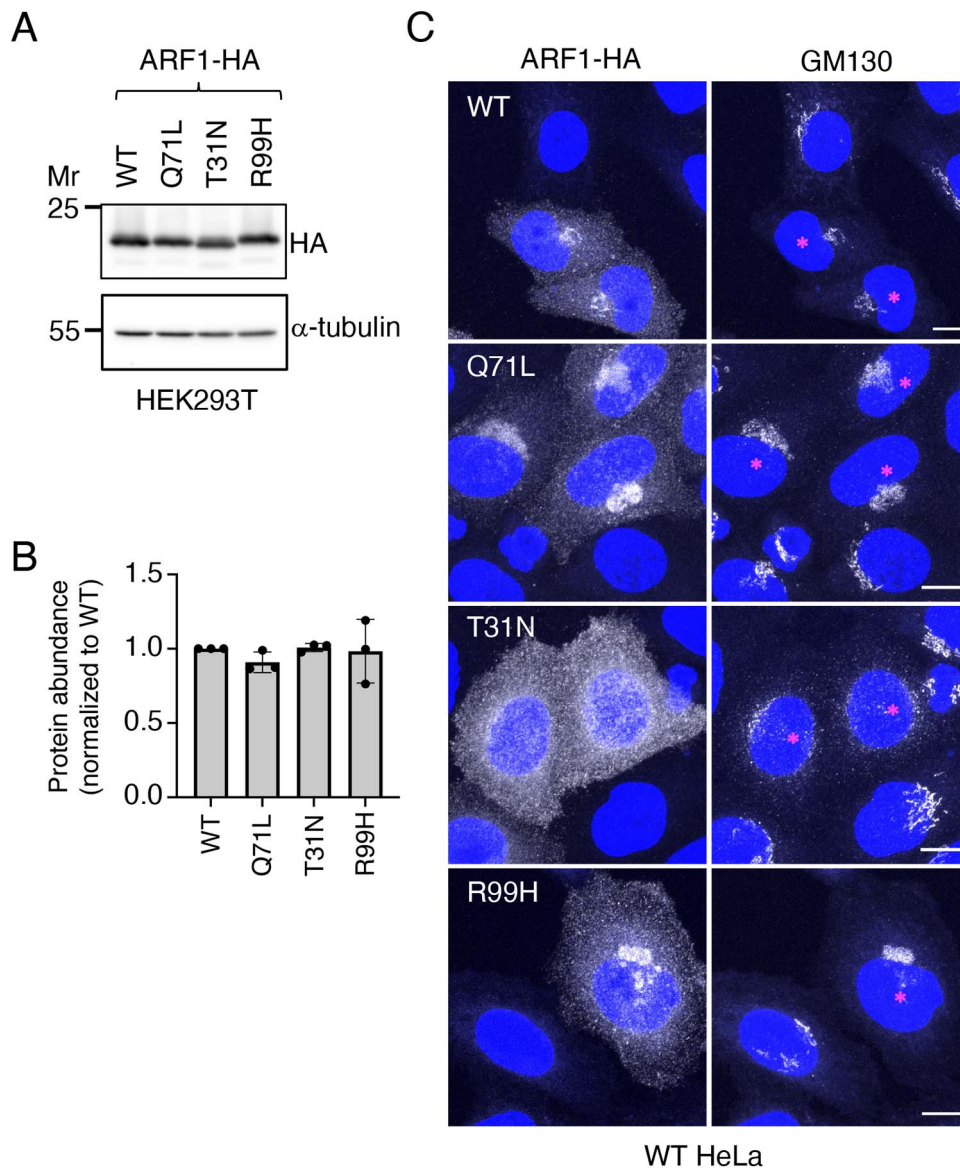
Figure 2. Characterization of WT and mutant ARF1-HA constructs expressed in human cells. (**A**) HEK293T cells were transfected with plasmids encoding WT, Q71L, T31N or R99H forms of ARF1-HA. Cells were lysed 24 h after transfection, and the lysates were analyzed by SDS-PAGE and immunoblotting with antibodies to the HA epitope and α-tubulin (loading control). The positions of molecular mass (Mr) markers (in kDa) are indicated on the left. (**B**) Quantification of the abundance of ARF1-HA forms normalized to the abundance of α-tubulin from three independent experiments such as that described in (A). WT abundance was defined as 1. Values are the mean ± SD. Statistical significance was calculated using one-way ANOVA with Dunnett's test. This test revealed no significant differences in expression levels. (**C**) Immunofluorescence microscopy of HeLa cells transfected with plasmids encoding WT, Q71L, T31N or R99H forms of ARF1-HA, and stained for the HA epitope (left panels; grayscale), GM130 (right panels; grayscale) and nuclei (DAPI; blue). Magenta asterisks on the right panels indicate cells expressing ARF1-HA proteins. Scale bars: 10 μm.

Taken together, the above results indicated that R99H is a gain-of-function variant that makes ARF1 hyperactive, likely interfering with cellular functions that require ARF1 cycling between GTP- and GDP-bound states.

Discussion

This work details the phenotype of a patient with an *ARF1*-related disorder and the pathogenetic mechanism behind her monoallelic *de novo* ARF1-R99H variant. To date, only a handful of subjects have been identified with *ARF1*-related disorders (8,43) and our report adds valuable phenotypic information toward the understanding of this disease. More importantly, our work demonstrates that the R99H variant in our patient causes disease through a constitutive-activation mechanism, wherein persistent ARF1 activity leads to Golgi and endosomal dysfunction with consequent alterations of CNS development, structure and function.

Previous studies of *ARF1*-related disorders identified five individuals with monoallelic *de novo* missense variants (one p.Y35H, one p.R99H and three p.K127E) (8,26,27) and two individuals (father and daughter) with a monoallelic inherited nonsense variant (p.Trp78X) in *ARF1* (43). All of these individuals exhibited a range of neurodevelopmental abnormalities. Although the depth of the clinical description and the specific clinical features varied among the different reports, phenotypes included DD, ID, spasticity, epilepsy, microcephaly, brain malformation, myelination delay, cortical thinning, vermian atrophy and PVNH (8,26,27,43). Our proband showed no evidence of the PVNH
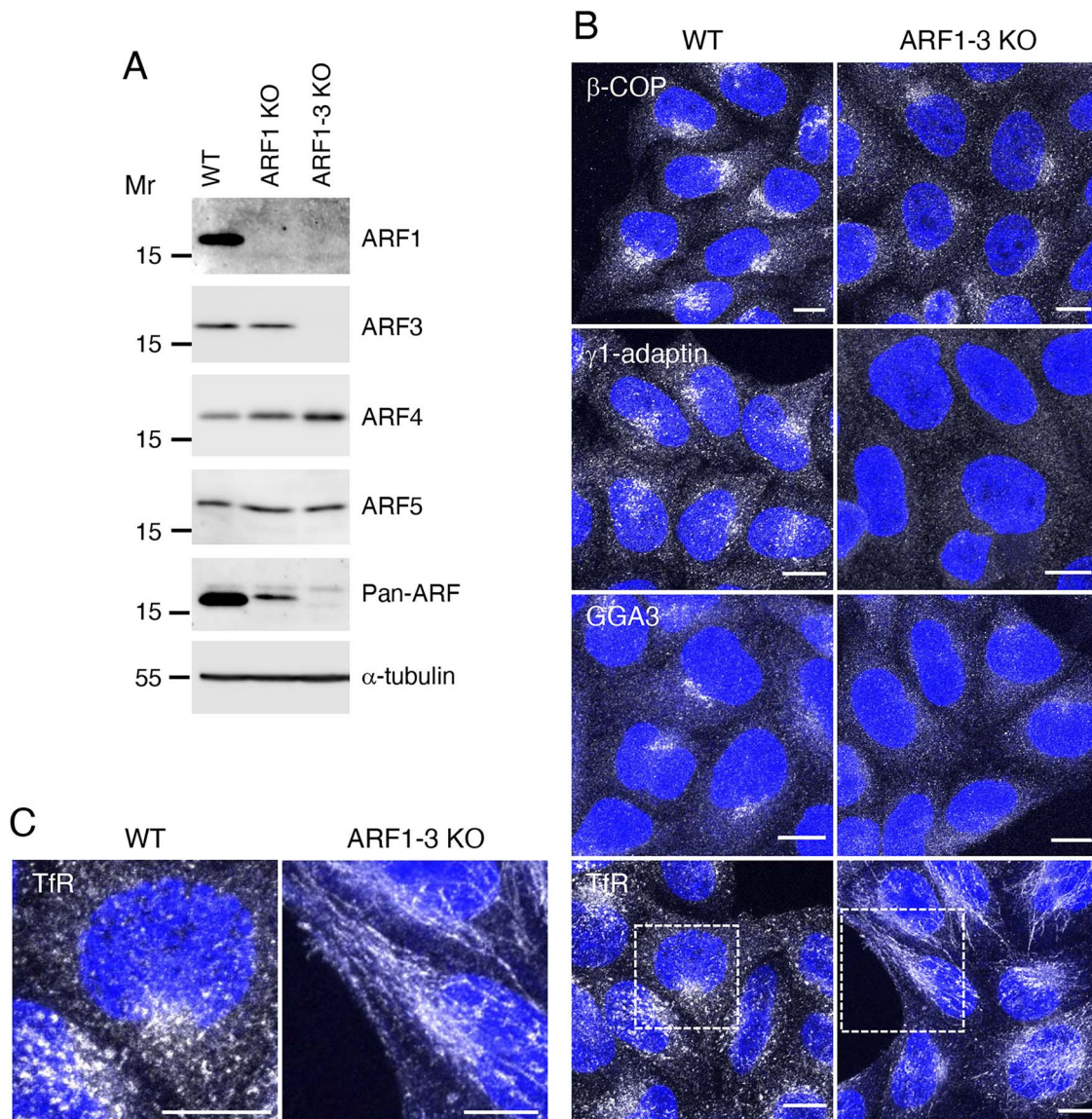
Figure 3. Characterization of ARF1–3-KO HeLa cells. (**A**) Single ARF1 KO and double ARF1–3 KO in HeLa cells was confirmed by SDS-PAGE and immunoblot analysis with antibodies to the proteins indicated on the right. *α*-tubulin was used as a loading control. Pan-ARF refers to an antibody that recognizes ARF1, ARF3, ARF5 and ARF6. The positions of molecular mass (Mr) markers (in kDa) are indicated on the left. (**B**) Immunofluorescence microscopy of WT and ARL1–3-KO HeLa cells immunostained for endogenous *β*-COP, *γ*1-adaptin, GGA3 or TfR (grayscale) and counterstained with DAPI (blue). Scale bars: 10 μm. (**C**) Magnified images of boxed areas in (B) (bottom panels). Scale bars: 10 μm.

observed in most individuals with *ARF1* variants, including the previously described individual with the same R99H variant (8). This observation indicates that PVNH may not be a consistent finding in all individuals with *ARF1*-related disorders and that these disorders may be variable as a result of genetic background or variants in ARF1-interacting proteins.

In principle, monoallelic variants could cause disease by haploinsufficiency, dominant-negative or constitutively active mechanisms. Most cases of *ARF1*-related disease described to date, including the previous R99H patient, have been attributed to haploinsufficiency (8,43); however, we show that R99H-ARF1 is hyperactive relative to WT-ARF1 in several assays. First, the expression of R99H-ARF1 in WT cells caused swelling of the Golgi apparatus. Second, rescue of ARF1–3-KO cells with R99H-ARF1 resulted in increased recruitment of ARF1-dependent coat proteins like COPI, AP-1 and GGA3 to the Golgi apparatus. Third, the expression of R99H-ARF1 caused swelling of recycling endosomes in both

ARF1–3-KO and WT cells. Fourth, R99H-ARF1 bound more strongly to its effector GGA3. Finally, the expression of R99H-ARF1 protected the Golgi apparatus from dispersal by the ARF1-inhibitor BFA. In all of these assays, R99H-ARF1 behaved like the well-characterized GTP-locked Q71L-ARF1 mutant, indicating that R99H-ARF1 is a gain-of-function variant that causes disease via a constitutively active mechanism.

Constitutive activation of ARF1 likely alters the dynamics of ARF1 effectors including coat proteins and lipid-modifying enzymes. These effectors bind more stably to constitutively active ARF1, thus interfering with the cycling of effectors that is required in various cellular processes. Indeed, previous studies showed that overexpression of the Q71L-ARF1 mutant inhibits ARF1-regulated processes such as ER-to-Golgi and intra-Golgi transport (5–7), mitotic Golgi disassembly, chromosome segregation and cytokinetic furrow ingression (44) and phagocytosis (45). Furthermore, ARF1 and/or its regulators have been implicated in neuronal
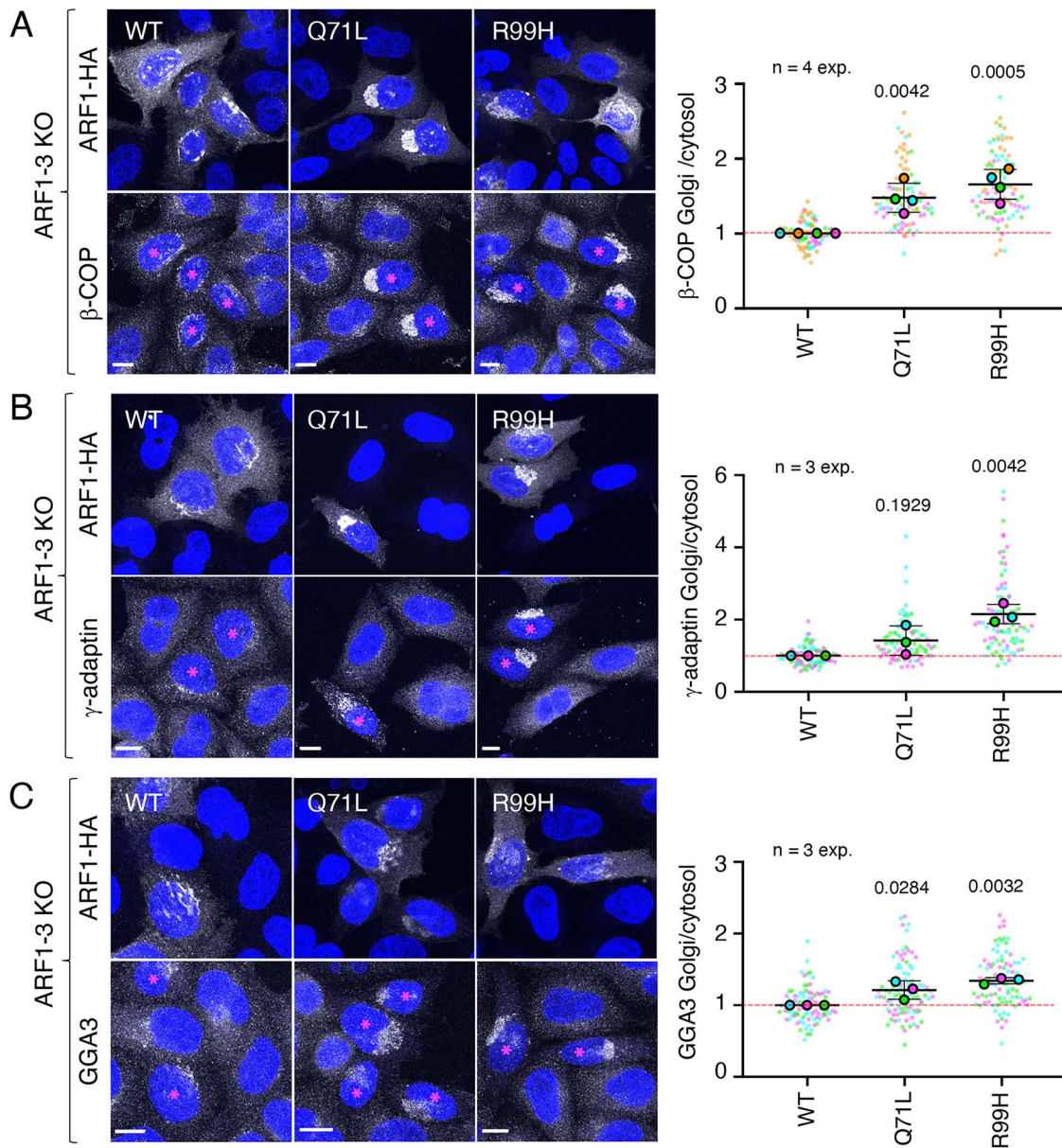
Figure 4. Recruitment of effectors by ARF1-HA mutants in ARF1–3-KO HeLa cells. (**A**–**C**) Immunofluorescence microscopy of ARF1–3-KO HeLa cells transfected with plasmids encoding WT, Q71L or R99H forms of ARF1-HA and immunostained for the HA epitope [top rows in (A–C)], β-COP [bottom row in (A)], γ1-adaptin [bottom row in (B)], GGA3 [bottom row in (C)] and nuclei (all panels, DAPI; blue). Single channels are shown in grayscale. Magenta asterisks on the bottom rows indicate cells expressing ARF1-HA mutants. Scale bars: 10 μm. Graphs on the right show the Golgi/cytosol ratios of the different effectors. Effector intensities were measured for 30 cells in each of three or four independent experiments (*n*). Data are represented as SuperPlots showing the individual data points in each experiment, the mean from each experiment and the mean ± SD of the means. The statistical significance of the differences relative to ARF1-WT-HA-expressing cells was determined using one-way ANOVA with Dunnett's test. *P*-values are indicated.

migration (46,47), dendrite formation, growth, morphogenesis and pruning (48–51), synaptic vesicle biogenesis and recycling (52–55) and synaptic plasticity (56); all processes that could be impaired by the expression of constitutively active ARF1. In fact, in both mammalian hippocampal neurons (48) and Drosophila sensory neurons (50), the expression of GTP-locked Q71L-ARF1 interferes with dendrite development. Finally, mutations in subunits of several ARF1 effectors such as the COPI (57), AP-1 (58–60), AP-3 (61,62) and AP-4 (63,64) coat proteins cause various neurodevelopmental disorders. Defects in these processes could play a role in the neurodevelopmental phenotype of the individuals with R99H-ARF1 or other constitutively activating variants.

A recent study identified two subjects with neurodevelopmental disorders possessing monoallelic *de novo* variants in *ARF3*, the ARF-family member that is most closely related to ARF1 (32). One of these subjects had a substitution (p.R99L) at the equivalent residue as our subject (32) (Fig. 1D). This individual was reported to have global DD, ID, hypotonia, dysmorphic facies, seizures, cerebellar hypoplasia and delayed myelination, but also no PVNH (32). Furthermore, an effector-binding assay showed that R99L-ARF3 binds more avidly to GGA1. These characteristics are similar to those of our subject's R99H-ARF1 variant, suggesting a similar pathogenetic mechanism for variants in both GTPases. These similarities can be explained by the high sequence homology of ARF1 and ARF3 (96% identity), their interactions with similar
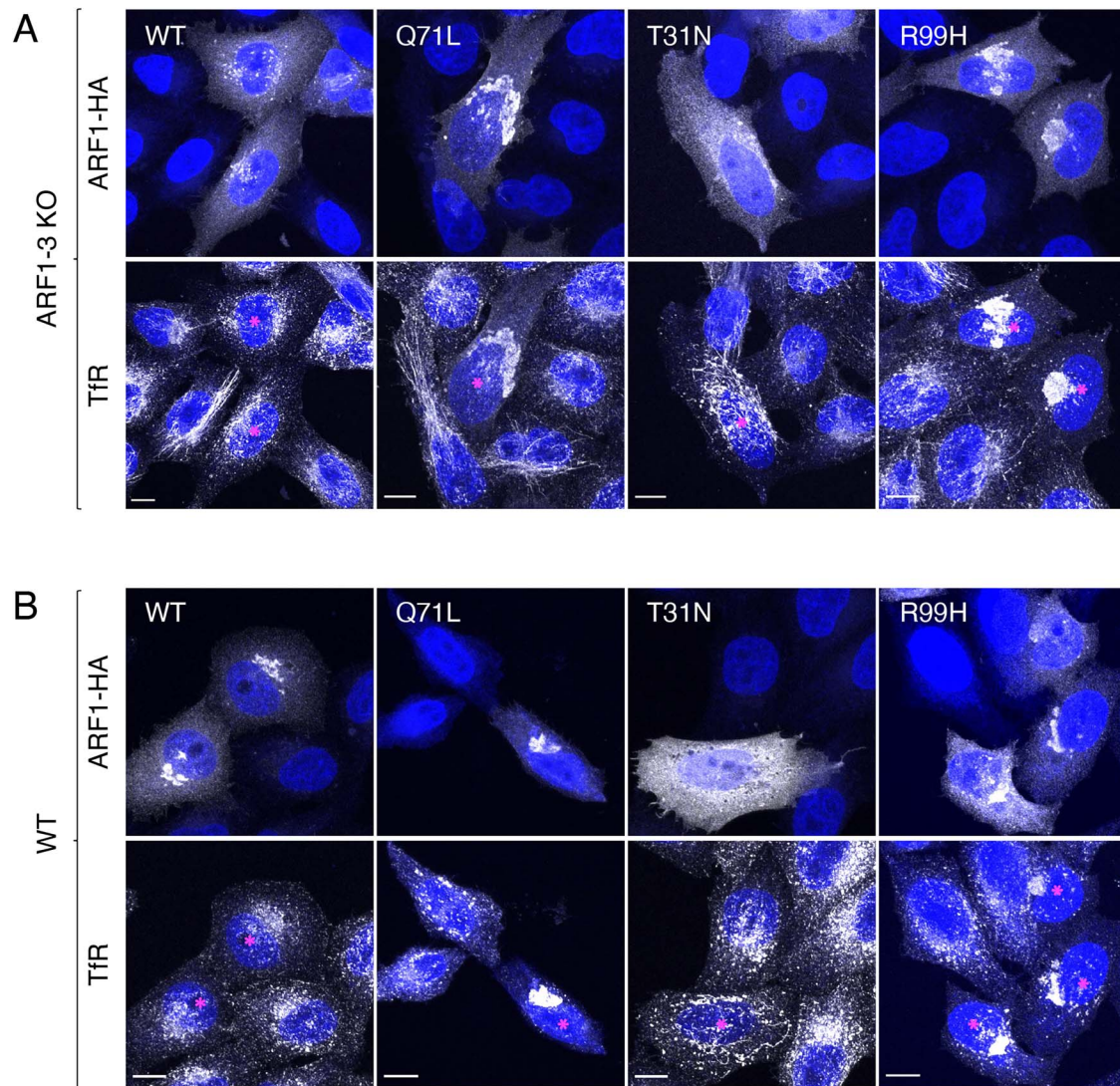
Figure 5. Perturbation of recycling endosomes by the expression of ARF1-HA mutants. (**A**, **B**) Immunofluorescence microscopy of ARF1–3-KO (A) and WT (B) HeLa cells transfected with plasmids encoding WT, Q71L, T31N or R99H forms of ARF1-HA, and stained for the HA epitope (top rows), TfR (bottom rows) and nuclei (DAPI; blue). Single channels are shown in grayscale. Magenta asterisks on the bottom panels indicate cells expressing ARF1-HA proteins. Scale bars: 10 μm.

sets of effectors and regulators and their overlapping (though not completely identical) functions (13–15,38,39,65–67).

Sakamoto *et al.* (32) proposed an explanation for the hyperactivity of the R99L-ARF3 variant, which we think also applies to the R99H-ARF1 variant described here. According to this explanation, R99 forms a salt bridge with D26 (Fig. 1B), which is conserved in both ARF1 and ARF3. Substitution of a histidine for an arginine at position 99 in ARF1 disrupts the interaction with D26, causing D26 to interfere with the ability of the catalytic Q71 residue to stabilize the attacking water during GTP hydrolysis.

Several other *ARF1* missense variants are listed in the ClinVar database (https://www.ncbi.nlm.nih.gov/clinvar/), but their clinical and functional significance remains to be established. One of these variants (c.295 C > T; ClinVar accession VCV001343805.1) encodes an R99C substitution. Based on the considerations discussed above, we expect this variant to also behave as a constitutively active form.

Because of the predominant localization of ARF1 to the Golgi apparatus, *ARF1*-related disorders could be classified as 'Golgipathies', a group of diseases caused by mutations in Golgi proteins (68). This classification encompasses different disorders, about half of which involve defects in the development of the central and/or peripheral nervous systems (68). Since ARF1 regulates various coat proteins, *ARF1*-related disorders could also fall under the classification of 'coatopathies', caused by mutations in coat proteins (16). Most coatopathies also exhibit a neurodevelopmental phenotype (16). Among the defects reported in Golgipathies and coatopathies are ID, epilepsy, spasticity, brain malformation, microcephaly, white matter defects and impaired neurogenesis and neuronal migration (16,68), all of which overlap with those seen with *ARF1*-variant patients.

Another potential mechanism for *ARF1*-related disorders is loss-of-function or partially inactivating mutations similar to one of the reported ARF3 subjects (D67V) (8). This subject was much more severely affected than the subject with the activating R99L variant. Extrapolation of this finding to subjects with ARF1-related disorders could mean there is a wide range of phenotypes among the different variants based on the identity of activating or inactivating variants. Furthermore, although it is difficult to clinically compare our R99H subject with the previously identified
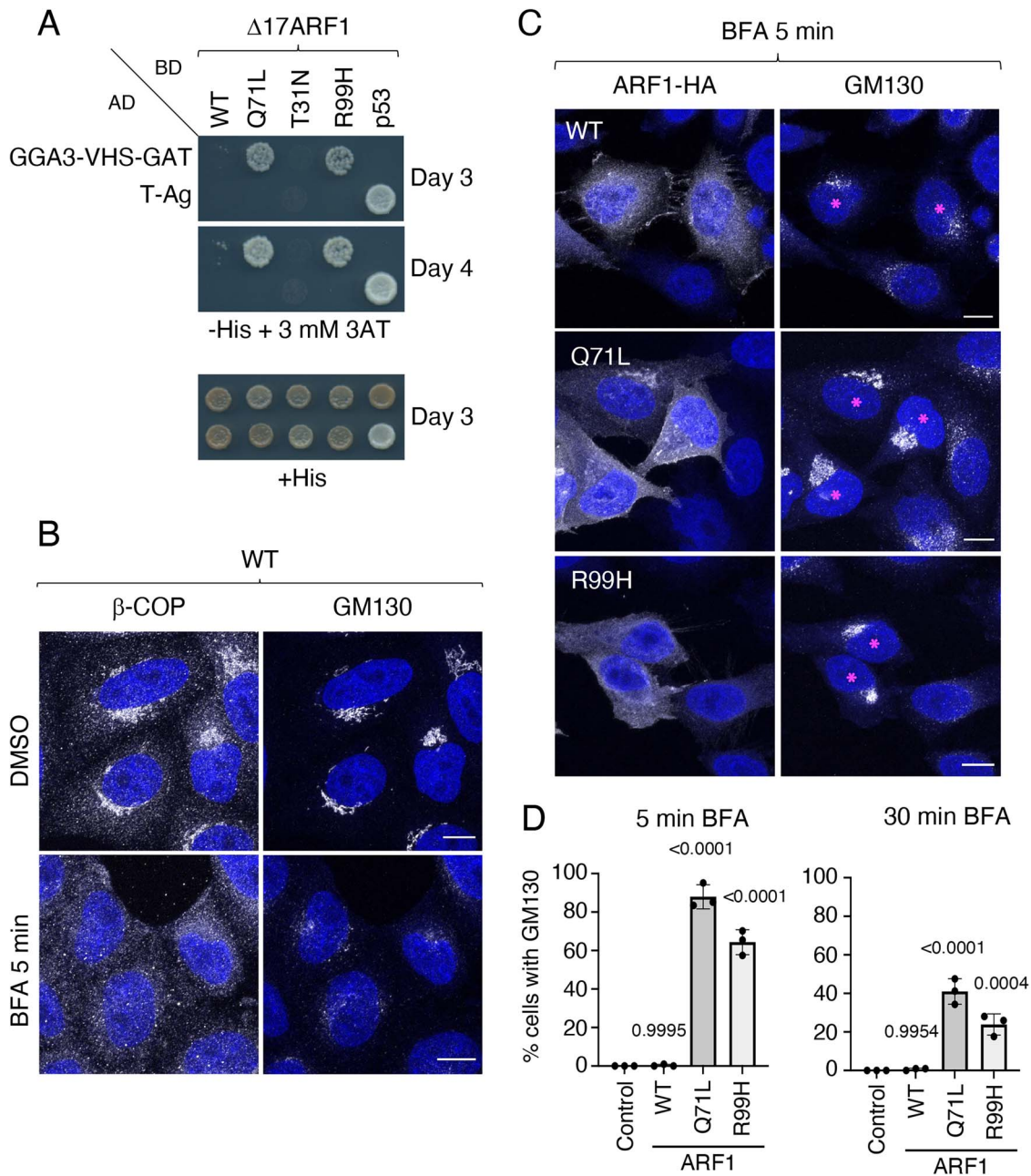
Figure 6. Evidence for hyperactivation of R99H-ARF1. (**A**) Yeast two-hybrid analysis of the interaction of (i) WT, Q71L, T31N or R99H forms of ARF1 lacking the N-terminal myristoylated α-helix (Δ17; deletion of the first 17 amino acid residues) fused to the Gal4 DNA BD, with (ii) the VHS-GAT domains of GGA3 fused to the Gal4 transcriptional AD. p53 and T antigen were used as controls. Yeast double transformants were suspended in sterile water at OD_{600} of 0.1, and 5 μl of the suspensions was spotted on two different plates and incubated at 30°C for up to 4 days. Growth in the absence of histidine and presence of 3 mM 3AT (−His +3 mM 3AT) is indicative of interactions. Growth in the presence of histidine (+His) is a control for viability and loading of yeast double transformants. (**B**) WT HeLa cells were treated with DMSO or 5 μg/ml BFA in DMSO for 5 min and immunostained for β-COP (left images), GM130 (right images) and nuclei (DAPI; blue). Single-channel images are shown in grayscale. Scale bars: 10 μm. (**C**) Immunofluorescence microscopy of WT HeLa cells transfected with plasmids encoding WT, Q71L or R99H forms of ARF1-HA, treated with 5 μg/ml BFA for 5 min and stained for the HA epitope (left images), GM130 (right images) and nuclei (DAPI; blue). Single-channel images are shown in grayscale. Magenta asterisks on the right panels indicate cells that express ARF1-HA proteins. Scale bars: 10 μm. (**D**) Quantification of the percentage of cells that retain compact Golgi morphology after 5 and 30 min of BFA treatment. Values are the mean ± SD from three independent experiments. More than 100 cells per sample were counted in each experiment. The statistical significance of the differences relative to untransfected cells was determined using one-way ANOVA with Dunnett's test. P-values are indicated.

R99H case (8) as a result of the latter's lack of in-depth clinical information, the absence of PVNH in our subject indicates that there could be a wide variability of phenotypes even among individuals with the same ARF1 genotype.

The demonstration of a gain-of-function mechanism for the R99H-ARF1 variant described here and the R99L-ARF3 variant reported previously (32) opens the possibility of other activating variants being identified and potentially being actionable with treatment by pharmacologic inhibition or silencing of ARF1 or ARF3. Although BFA inhibits both ARF1 and ARF3, it is too toxic for human use (69,70); however, the synthesis or isolation of new BFA analogs (71) could lead to the identification of compounds with a safer pharmacological profile. Antisense oligonucleotides could be another therapeutic intervention to silence these hyperactive

ARF variants (72). Of course, much of the efficacy of any potential therapeutic intervention depends on whether these are static or progressive disorders that are amenable to reversal, and how much of the patients' structural brain abnormalities play in their phenotype. Nevertheless, understanding these mechanisms and etiologies of disease are important first steps in determining what can and cannot be rescued.

Materials and Methods
Standard protocol approvals, registrations and patient consents
Patient research protocols were approved through the institutional review board, and the family gave informed consent (CSMC IRB protocol Pro00037131).

Genetic evaluation
Genomic DNA was extracted from blood, and exome sequencing was performed as per previous protocols (GeneDx, Gaithersburg, MD) (73).

Antibodies
The following primary antibodies (supplier and catalog number in parentheses) were used for immunoblotting and/or immunofluorescence microscopy: mouse HRP-conjugated anti-α-tubulin (Santa Cruz Biotechnology, DM1A), rat anti-HA epitope (Roche, 3F10), mouse anti-GM130 (BD Biosciences, 610823), mouse anti-γ1-adaptin (BD Biosciences, 610385), mouse anti-GGA3 (BD Biosciences, 612310), rabbit anti-β-COP (Thermo Fisher Scientific, PA1-061), mouse anti-TfR (Santa Cruz, sc-65882), mouse anti-ARF1 (Santa Cruz, sc-53168), mouse anti-ARF3 (Santa Cruz, sc-135841), rabbit anti-ARF4 (Proteintech, 11673-1-AP), mouse anti-ARF5 (Santa Cruz, sc-81 893), mouse anti-pan-ARF (Thermo Fisher Scientific, MA3-060), HRP-conjugated goat anti-rabbit IgG (Jackson ImmunoResearch, 111-035-003), HRP-conjugated goat anti-rat IgG (Jackson ImmunoResearch, 112-035-143), HRP-conjugated goat anti-mouse IgG (Jackson ImmunoResearch, 715-035-150), Alexa Fluor 594 donkey anti-rat IgG (Thermo Fisher Scientific, A21209), Alexa Fluor 488 donkey anti-mouse IgG (Thermo Fisher Scientific, A21202) and Alexa Fluor 488 donkey anti-rabbit IgG (Thermo Fisher Scientific, A21206).

Recombinant DNAs
Human ARF1 complementary DNA was obtained from the ORFeome v8.1 collection (Dharmacon). Q71L- and T31N-ARF1 cDNAs were described previously (13). cDNAs encoding C-terminally HA-tagged ARF1 (WT, Q71L or T31N) were amplified by PCR using the ARF1 cDNAs as templates and the following pairs of oligonucleotides (restriction enzyme sites are underlined): forward primer, GG<u>GGT ACC</u>GC CACCA TGGGG AACAT CTTCG CCAA; reverse primer, AGAGT <u>CGCGG CCGC</u>T TCAAG CGTAG TCTGG GACGT CGTAT GGGTA GGTGG CGACC GGTGG ATCCC GCTTC TGGTT CCGGA GCTGA T. The resulting amplicons were subcloned into *KpnI-NotI*-digested pEGFP-N1 vector (Clontech). As a result, the EGFP sequence in the vector was replaced with an HA epitope sequence. The R99H mutation was introduced into ARF1-HA by site-directed mutagenesis using the QuikChange XL Site-Directed Mutagenesis Kit (Agilent, 200516) and the following pairs of oligonucleotides: forward primer, GGACAGCAATGACAGAGAGCATGTGAACGAGGCCCGTGAGG; reverse primer, CCTCACGGGCCTCGTTCACATGCTCTCTGTCATTGCTGTCC. The plasmids pGBKT7-ARF1Δ17-WT, pGBKT7-ARF1Δ17-Q71L and pGBKT7-ARF1Δ17-T31N were described previously (13). A PCR amplicon of ARF1Δ17-R99H was generated using forward

primer GCC<u>GA ATTC</u>A TGCGC ATCCT CATGG TGGG and reverse primer, GAC<u>GG ATCC</u>C TACTT CTGGT TCCGG AGCTG (restriction enzyme sites are underlined), and subcloned into *EcoRI-BamHI*-digested pGBKT7 vector (Clontech). pGAD424-GGA3-VHS-GAT was described previously (15).

Cell culture and transfection
HeLa (ATCC, CCL-2) and HEK293T (ATCC, CRL-3216) cells were maintained in Dulbecco's Modified Eagle's Medium (Quality Biological, 112-319-101) supplemented with 10% fetal bovine serum (Corning, 35-011-CV), MycoZap Plus-CL (Lonza, VZA-2012) at 5% CO_2 and 37°C. Lipofectamine 2000 (ThermoFisher, 11668019) was used for transfections according to the manufacturer's protocol. Cells were lysed, or fixed and imaged ~24 h after transfection.

Immunoblotting
Cells were trypsinized, collected in 1.5 ml tubes, washed with PBS once and lysed in 1% Triton X-100, 50 mM Tris-HCl pH 7.4, 150 mM NaCl and cOmplete EDTA-free Protease Inhibitor Cocktail (Roche, 11873580001). Laemmli SDS-PAGE sample buffer (Bio-Rad, #161-0747) containing 2.5% 2-mercaptoethanol was added to the lysate, and the lysate was incubated for 5 min at 98°C. Proteins were resolved by SDS-PAGE and subsequently transferred to nitro-cellulose membranes. Membranes were blocked for 0.5–1 h with 3% nonfat milk (Bio-Rad, #1706404) in TBS-T (TBS supplemented with 0.05% Tween 20; Sigma-Aldrich, P9416-100ML) before incubation with primary antibody diluted in TBS-T with 3% nonfat milk. Membranes were washed three times for 20 min in TBS-T and incubated for 2–3 h in HRP-conjugated secondary antibody (1:5000) diluted in TBS-T with 3% nonfat milk. Membranes were washed three times in TBS-T and visualized using Clarity ECL Western Blot substrate (Bio-Rad, #1705061).

Immunofluorescence microscopy
Cells were plated onto fibronectin-coated cover glasses, transfected with Lipofectamine 2000 according to the manufacturer's instructions and fixed with 4% paraformaldehyde in PBS. Cells were then permeabilized and blocked simultaneously with 0.1% saponin (Sigma-Aldrich) and 1% BSA in PBS for 30 min at room temperature. Primary antibodies were diluted in the same buffer and incubated on cells for 90 min at room temperature. Alexa Fluor secondary antibodies were diluted in the same buffer containing DAPI (Thermo Fisher Scientific, D1306), and cells were incubated for 1 h at room temperature. The coverslips were mounted on glass slides using ProLong Gold Antifade (Thermo Fisher Scientific, P36934) and the cells were imaged on a confocal microscope (LSM780, Carl Zeiss) with an oil-immersion 63×/1.40 NA Plan-Apochromat Oil DIC M27 objective lens (Carl Zeiss). Image settings (i.e. gain, laser power and pinhole) were kept constant for comparison. Images were acquired using Zeiss ZEN Black software (Carl Zeiss) and processed with Fiji (https://imagej.net/software/fiji/), including brightness adjustment, contrast adjustment, channel merging and cropping.

CRISPR-Cas9 KO
ARF1-KO and ARF1–3-DKO HeLa cells were generated using CRISPR-Cas9 (74). The targeting sequences for human *ARF1* (5′-AAAAG AAATG CGCAT CCTCA/CTTAA GCTTG TAGAG GATCG-3′) and human *ARF3* (5′-AGAAC ATCAG CTTTA CAGTG/AGAGG GGTCG AATCT TGTCC-3′) were separately cloned into pSpCas9 (BB)-2A-GFP plasmid (Addgene, 48138, deposited by Feng Zhang, Massachusetts Institute of Technology, Cambridge, MA). For ARF1-KO, HeLa cells were transfected with two plasmids containing gRNAs targeting *ARF1*. GFP-positive cells were isolated by flow

cytofluorometry after 24 h and single-cell cloned in 96-well plates. KO of ARF1 was confirmed by immunoblotting. The resulting ARF1-KO HeLa cells were further transfected with two plasmids containing gRNAs targeting *ARF3*, GFP-positive cells were isolated and KO of ARF3 was confirmed by immunoblotting.

Yeast two-hybrid assays

Yeast two-hybrid assays were performed using pGBKT7 vectors that harbor WT and mutant ARF1 lacking the N-terminal myristoylated α-helix (Δ17; deletion of the first 17 amino acid residues) and pGAD424-GGA3-VHS-GAT. The yeast strain (AH109), selection medium, culture conditions and transformation protocol were as previously described (75).

BFA treatment

WT HeLa cells were transfected with plasmids encoding ARF1-HA (WT, Q71L or R99H). At 24 h after transfection, cells were treated with 5 μg/ml BFA (BioLegend, 420601) for 5 or 30 min in a 5% CO_2, 37°C incubator. The cells were fixed, immunostained as described above and examined for ARF1-HA localization and morphology of the Golgi apparatus.

Quantification and statistics

Quantification of the abundance of WT, T31N, Q71L and R99H variants of ARF1-HA in immunoblots (Fig. 2A) was performed using the function 'Gels' in Fiji (https://imagej.net/software/fiji/). The band intensities of ARF1-HA were normalized to the intensities of α-tubulin in each lane, and values for T31N-ARF1, Q71L-ARF1 and R99H-ARF1 were normalized to those of WT ARF1.

The intensity of effectors recruited by ARF1-HA variants to the Golgi apparatus (Fig. 4A–C) was measured using the function 'Measure' in Fiji. Maximum intensity projections of z-stack images were acquired for each condition, and the Golgi apparatus in each cell was selected by drawing a region of interest encircling the ARF1-HA signal on the Golgi apparatus with the selection brush tool. Part of the cytosol in each cell was randomly selected with the same tool, and mean intensities of effectors on the Golgi apparatus and those in the cytosol were measured. The mean intensities of effectors on the Golgi apparatus were divided by the mean intensities of effectors in the cytosol.

Quantification of the percentage of cells exhibiting normal Golgi morphology (Fig. 6D) was performed by counting >100 ARF1-HA protein-expressing cells per sample per experiment in three independent experiments. Percentages were calculated using Excel (Microsoft).

Data are presented as means ± SD or SuperPlots (76). Statistical significance was calculated using one-way ANOVA followed by multiple comparisons using Dunnett's test (Prism 9 for macOS). All graphs were drawn using Prism 9 for macOS and *P*-values are indicated in each graph.

Acknowledgements

Funding

References

1. Donaldson, J.G. and Jackson, C.L. (2011) ARF family G proteins and their regulators: roles in membrane transport, development and disease. *Nat. Rev. Mol. Cell Biol.*, **12**, 362–375.

2. Sztul, E., Chen, P.W., Casanova, J.E., Cherfils, J., Dacks, J.B., Lambright, D.G., Lee, F.S., Randazzo, P.A., Santy, L.C., Schurmann, A. *et al.* (2019) ARF GTPases and their GEFs and GAPs: concepts and challenges. *Mol. Biol. Cell*, **30**, 1249–1271.

3. Itzhak, D.N., Tyanova, S., Cox, J. and Borner, G.H. (2016) Global, quantitative and dynamic mapping of protein subcellular localization. *eLife*, **5**, e16950.

4. Peyroche, A., Antonny, B., Robineau, S., Acker, J., Cherfils, J. and Jackson, C.L. (1999) Brefeldin A acts to stabilize an abortive ARF-GDP-Sec7 domain protein complex: involvement of specific residues of the Sec7 domain. *Mol. Cell*, **3**, 275–285.

5. Dascher, C. and Balch, W.E. (1994) Dominant inhibitory mutants of ARF1 block endoplasmic reticulum to Golgi transport and trigger disassembly of the Golgi apparatus. *J. Biol. Chem.*, **269**, 1437–1448.

6. Teal, S.B., Hsu, V.W., Peters, P.J., Klausner, R.D. and Donaldson, J.G. (1994) An activating mutation in ARF1 stabilizes coatomer binding to Golgi membranes. *J. Biol. Chem.*, **269**, 3135–3138.

7. Zhang, C.J., Rosenwald, A.G., Willingham, M.C., Skuntz, S., Clark, J. and Kahn, R.A. (1994) Expression of a dominant allele of human ARF1 inhibits membrane traffic in vivo. *J. Cell Biol.*, **124**, 289–300.

8. Ge, X., Gong, H., Dumas, K., Litwin, J., Phillips, J.J., Waisfisz, Q., Weiss, M.M., Hendriks, Y., Stuurman, K.E., Nelson, S.F. *et al.* (2016) Missense-depleted regions in population exomes implicate ras superfamily nucleotide-binding protein alteration in patients with brain malformation. *NPJ Genom. Med.*, **1**, 16036.

9. Serafini, T., Orci, L., Amherdt, M., Brunner, M., Kahn, R.A. and Rothman, J.E. (1991) ADP-ribosylation factor is a subunit of the coat of Golgi-derived COP-coated vesicles: a novel role for a GTP-binding protein. *Cell*, **67**, 239–253.

10. Donaldson, J.G., Cassel, D., Kahn, R.A. and Klausner, R.D. (1992) ADP-ribosylation factor, a small GTP-binding protein, is required for binding of the coatomer protein beta-COP to Golgi membranes. *Proc. Natl. Acad. Sci. U. S. A.*, **89**, 6408–6412.

11. Traub, L.M., Ostrom, J.A. and Kornfeld, S. (1993) Biochemical dissection of AP-1 recruitment onto Golgi membranes. *J. Cell Biol.*, **123**, 561–573.

12. Ooi, C.E., Dell'Angelica, E.C. and Bonifacino, J.S. (1998) ADP-ribosylation factor 1 (ARF1) regulates recruitment of the AP-3 adaptor complex to membranes. *J. Cell Biol.*, **142**, 391–402.

13. Boehm, M., Aguilar, R.C. and Bonifacino, J.S. (2001) Functional and physical interactions of the adaptor protein complex AP-4 with ADP-ribosylation factors (ARFs). *EMBO J.*, **20**, 6265–6276.

14. Boman, A.L., Zhang, C., Zhu, X. and Kahn, R.A. (2000) A family of ADP-ribosylation factor effectors that can alter membrane transport through the trans-Golgi. *Mol. Biol. Cell*, **11**, 1241–1255.

15. Dell'Angelica, E.C., Puertollano, R., Mullins, C., Aguilar, R.C., Vargas, J.D., Hartnell, L.M. and Bonifacino, J.S. (2000) GGAs: a family of ADP ribosylation factor-binding proteins related to adaptors and associated with the Golgi complex. *J. Cell Biol.*, **149**, 81–94.

16. Dell'Angelica, E.C. and Bonifacino, J.S. (2019) Coatopathies: genetic disorders of protein coats. *Annu. Rev. Cell Dev. Biol.*, **35**, 131–168.

17. Sanger, A., Hirst, J., Davies, A.K. and Robinson, M.S. (2019) Adaptor protein complexes and disease at a glance. *J. Cell Sci.*, **132**, jcs222992.

18. Wong, D.H. and Brodsky, F.M. (1992) 100-kD proteins of Golgi- and *trans*-Golgi network-associated coated vesicles have related but distinct membrane binding properties. *J. Cell Biol.*, **117**, 1171–1179.

19. Dell'Angelica, E.C., Ohno, H., Ooi, C.E., Rabinovich, E., Roche, K.W. and Bonifacino, J.S. (1997) AP-3: an adaptor-like protein complex with ubiquitous expression. *EMBO J.*, **16**, 917–928.

20. Simpson, F., Peden, A.A., Christopoulou, L. and Robinson, M.S. (1997) Characterization of the adaptor-related protein complex, AP-3. *J. Cell Biol.*, **137**, 835–845.

21. Dell'Angelica, E.C., Mullins, C. and Bonifacino, J.S. (1999) AP-4, a novel protein complex related to clathrin adaptors. *J. Biol. Chem.*, **274**, 7278–7285.

22. Hirst, J., Bright, N.A., Rous, B. and Robinson, M.S. (1999) Characterization of a fourth adaptor-related protein complex. *Mol. Biol. Cell*, **10**, 2787–2802.

23. Lippincott-Schwartz, J., Yuan, L.C., Bonifacino, J.S. and Klausner, R.D. (1989) Rapid redistribution of Golgi proteins into the ER in cells treated with brefeldin A: evidence for membrane cycling from Golgi to ER. *Cell*, **56**, 801–813.

24. Ward, T.H., Polishchuk, R.S., Caplan, S., Hirschberg, K. and Lippincott-Schwartz, J. (2001) Maintenance of Golgi structure and function depends on the integrity of ER export. *J. Cell Biol.*, **155**, 557–570.

25. Hayakawa, N., Ogoh, H., Sumiyoshi, M., Matsui, Y., Nishikawa, S., Miyamoto, K., Maede, Y., Kiyonari, H., Suzuki, M. and Watanabe, T. (2014) The ADP-ribosylation factor 1 gene is indispensable for mouse embryonic development after implantation. *Biochem. Biophys. Res. Commun.*, **453**, 748–753.

26. Heinzen, E.L., O'Neill, A.C., Zhu, X., Allen, A.S., Bahlo, M., Chelly, J., Chen, M.H., Dobyns, W.B., Freytag, S., Guerrini, R. *et al.* (2018) De novo and inherited private variants in MAP1B in periventricular nodular heterotopia. *PLoS Genet.*, **14**, e1007281.

27. Monies, D., Abouelhoda, M., Assoum, M., Moghrabi, N., Rafiullah, R., Almontashiri, N., Alowain, M., Alzaidan, H., Alsayed, M., Subhani, S. *et al.* (2019) Lessons learned from large-scale, first-tier clinical exome sequencing in a highly consanguineous population. *Am. J. Hum. Genet.*, **105**, 879.

28. Click, E.S., Stearns, T. and Botstein, D. (2002) Systematic structure-function analysis of the small GTPase Arf1 in yeast. *Mol. Biol. Cell*, **13**, 1652–1664.

29. Serbzhinskiy, D.A., Clifton, M.C., Sankaran, B., Staker, B.L., Edwards, T.E. and Myler, P.J. (2015) Structure of an ADP-ribosylation factor, ARF1, from Entamoeba histolytica bound to Mg(2+)-GDP. *Acta Crystallogr. F Struct. Biol. Commun.*, **71**, 594–599.

30. Shiba, T., Kawasaki, M., Takatsu, H., Nogi, T., Matsugaki, N., Igarashi, N., Suzuki, M., Kato, R., Nakayama, K. and Wakatsuki, S. (2003) Molecular mechanism of membrane recruitment of GGA by ARF in lysosomal protein transport. *Nat. Struct. Biol.*, **10**, 386–393.

31. Goldberg, J. (1998) Structural basis for activation of ARF GTPase: mechanisms of guanine nucleotide exchange and GTP-myristoyl switching. *Cell*, **95**, 237–248.

32. Sakamoto, M., Sasaki, K., Sugie, A., Nitta, Y., Kimura, T., Gursoy, S., Cinleti, T., Iai, M., Sengoku, T., Ogata, K. *et al.* (2021) De novo ARF3 variants cause neurodevelopmental disorder with brain abnormality. *Hum. Mol. Genet.*, **31**, 69–81.

33. Stamnes, M.A. and Rothman, J.E. (1993) The binding of AP-1 clathrin adaptor particles to Golgi membranes requires ADP-ribosylation factor, a small GTP-binding protein. *Cell*, **73**, 999–1005.

34. Hirst, J., Lui, W.W., Bright, N.A., Totty, N., Seaman, M.N. and Robinson, M.S. (2000) A family of proteins with gamma-adaptin and VHS domains that facilitate trafficking between the *trans*-Golgi network and the vacuole/lysosome. *J. Cell Biol.*, **149**, 67–80.

35. Lippincott-Schwartz, J., Yuan, L., Tipper, C., Amherdt, M., Orci, L. and Klausner, R.D. (1991) Brefeldin A's effects on endosomes, lysosomes, and the TGN suggest a general mechanism for regulating organelle structure and membrane traffic. *Cell*, **67**, 601–616.

36. Wood, S.A., Park, J.E. and Brown, W.J. (1991) Brefeldin A causes a microtubule-mediated fusion of the *trans*-Golgi network and early endosomes. *Cell*, **67**, 591–600.

37. Shin, H.W., Morinaga, N., Noda, M. and Nakayama, K. (2004) BIG2, a guanine nucleotide exchange factor for ADP-ribosylation factors: its localization to recycling endosomes and implication in the endosome integrity. *Mol. Biol. Cell*, **15**, 5283–5294.

38. Volpicelli-Daley, L.A., Li, Y., Zhang, C.J. and Kahn, R.A. (2005) Isoform-selective effects of the depletion of ADP-ribosylation factors 1-5 on membrane traffic. *Mol. Biol. Cell*, **16**, 4495–4508.

39. Kondo, Y., Hanai, A., Nakai, W., Katoh, Y., Nakayama, K. and Shin, H.W. (2012) ARF1 and ARF3 are required for the integrity of recycling endosomes and the recycling pathway. *Cell Struct. Funct.*, **37**, 141–154.

40. Nakai, W., Kondo, Y., Saitoh, A., Naito, T., Nakayama, K. and Shin, H.W. (2013) ARF1 and ARF4 regulate recycling endosomal morphology and retrograde transport from endosomes to the Golgi apparatus. *Mol. Biol. Cell*, **24**, 2570–2581.

41. Lippincott-Schwartz, J., Donaldson, J.G., Schweizer, A., Berger, E.G., Hauri, H.P., Yuan, L.C. and Klausner, R.D. (1990) Microtubule-dependent retrograde transport of proteins into the ER in the presence of brefeldin A suggests an ER recycling pathway. *Cell*, **60**, 821–836.

42. Donaldson, J.G., Lippincott-Schwartz, J., Bloom, G.S., Kreis, T.E. and Klausner, R.D. (1990) Dissociation of a 110-kD peripheral membrane protein from the Golgi apparatus is an early event in brefeldin A action. *J. Cell Biol.*, **111**, 2295–2306.

43. Gana, S., Casella, A., Cociglio, S., Tartara, E., Rognone, E., Giorgio, E., Pichiecchio, A., Orcesi, S. and Valente, E.M. (2022) ARF1 haploinsufficiency causes periventricular nodular heterotopia with variable clinical expressivity. *J. Med. Genet.*, **59**, 781–784.

44. Altan-Bonnet, N., Phair, R.D., Polishchuk, R.S., Weigert, R. and Lippincott-Schwartz, J. (2003) A role for Arf1 in mitotic Golgi disassembly, chromosome segregation, and cytokinesis. *Proc. Natl. Acad. Sci. U. S. A.*, **100**, 13314–13319.

45. Beemiller, P., Hoppe, A.D. and Swanson, J.A. (2006) A phosphatidylinositol-3-kinase-dependent signal transition regulates ARF1 and ARF6 during Fcgamma receptor-mediated phagocytosis. *PLoS Biol.*, **4**, e162.

46. Zhang, J., Neal, J., Lian, G., Hu, J., Lu, J. and Sheen, V. (2013) Filamin A regulates neuronal migration through brefeldin A-inhibited guanine exchange factor 2-dependent Arf1 activation. *J. Neurosci.*, **33**, 15735–15746.

47. Sheen, V.L., Ganesh, V.S., Topcu, M., Sebire, G., Bodell, A., Hill, R.S., Grant, P.E., Shugart, Y.Y., Imitola, J., Khoury, S.J., Guerrini, R. and Walsh, C.A. (2004) Mutations in ARFGEF2 implicate vesicle trafficking in neural progenitor proliferation and migration in the human cerebral cortex. *Nat. Genet.*, **36**, 69–76.

48. Horton, A.C., Racz, B., Monson, E.E., Lin, A.L., Weinberg, R.J. and Ehlers, M.D. (2005) Polarized secretory trafficking directs cargo for asymmetric dendrite growth and morphogenesis. *Neuron*, **48**, 757–771.

49. Arnold, M., Cross, R., Singleton, K.S., Zlatic, S., Chapleau, C., Mullin, A.P., Rolle, I., Moore, C.C., Theibert, A., Pozzo-Miller, L., Faundez, V. and Larimore, J. (2016) The endosome localized Arf-GAP AGAP1 modulates dendritic spine morphology downstream of the neurodevelopmental disorder factor dysbindin. *Front. Cell. Neurosci.*, **10**, 218.

50. Wang, Y., Zhang, H., Shi, M., Liou, Y.C., Lu, L. and Yu, F. (2017) Sec71 functions as a GEF for the small GTPase Arf1 to govern dendrite pruning of Drosophila sensory neurons. *Development*, **144**, 1851–1862.

51. Ito, A., Fukaya, M., Saegusa, S., Kobayashi, E., Sugawara, T., Hara, Y., Yamauchi, J., Okamoto, H. and Sakagami, H. (2018) Pallidin is a novel interacting protein for cytohesin-2 and regulates the early endosomal pathway and dendritic formation in neurons. *J. Neurochem.*, **147**, 153–177.

52. Faundez, V., Horng, J.T. and Kelly, R.B. (1997) ADP ribosylation factor 1 is required for synaptic vesicle budding in PC12 cells. *J. Cell Biol.*, **138**, 505–515.

53. Glyvuk, N., Tsytsyura, Y., Geumann, C., D'Hooge, R., Huve, J., Kratzke, M., Baltes, J., Boening, D., Klingauf, J. and Schu, P. (2010) AP-1/sigma1B-adaptin mediates endosomal synaptic vesicle recycling, learning and memory. *EMBO J.*, **29**, 1318–1330.

54. Cheung, G. and Cousin, M.A. (2012) Adaptor protein complexes 1 and 3 are essential for generation of synaptic vesicles from activity-dependent bulk endosomes. *J. Neurosci.*, **32**, 6014–6023.

55. Ramperez, A., Sanchez-Prieto, J. and Torres, M. (2017) Brefeldin A sensitive mechanisms contribute to endocytotic membrane retrieval and vesicle recycling in cerebellar granule cells. *J. Neurochem.*, **141**, 662–675.

56. Rocca, D.L., Amici, M., Antoniou, A., Blanco Suarez, E., Halemani, N., Murk, K., McGarvey, J., Jaafari, N., Mellor, J.R., Collingridge, G.L. and Hanley, J.G. (2013) The small GTPase Arf1 modulates Arp2/3-mediated actin polymerization via PICK1 to regulate synaptic plasticity. *Neuron*, **79**, 293–307.

57. Izumi, K., Brett, M., Nishi, E., Drunat, S., Tan, E.S., Fujiki, K., Lebon, S., Cham, B., Masuda, K., Arakawa, M. *et al.* (2016) ARCN1 mutations cause a recognizable craniofacial syndrome due to COPI-mediated transport defects. *Am. J. Hum. Genet.*, **99**, 451–459.

58. Montpetit, A., Cote, S., Brustein, E., Drouin, C.A., Lapointe, L., Boudreau, M., Meloche, C., Drouin, R., Hudson, T.J., Drapeau, P. *et al.* (2008) Disruption of AP1S1, causing a novel neurocutaneous syndrome, perturbs development of the skin and spinal cord. *PLoS Genet.*, **4**, e1000296.

59. Usmani, M.A., Ahmed, Z.M., Magini, P., Pienkowski, V.M., Rasmussen, K.J., Hernan, R., Rasheed, F., Hussain, M., Shahzad, M., Lanpher, B.C. *et al.* (2021) De novo and bi-allelic variants in AP1G1 cause neurodevelopmental disorder with developmental delay, intellectual disability, and epilepsy. *Am. J. Hum. Genet.*, **108**, 1330–1341.

60. Saillour, Y., Zanni, G., Des Portes, V., Heron, D., Guibaud, L., Iba-Zizen, M.T., Pedespan, J.L., Poirier, K., Castelnau, L., Julien, C. *et al.* (2007) Mutations in the AP1S2 gene encoding the sigma 2 subunit of the adaptor protein 1 complex are associated with syndromic X-linked mental retardation with hydrocephalus and calcifications in basal ganglia. *J. Med. Genet.*, **44**, 739–744.

61. Mohammed, M., Al-Hashmi, N., Al-Rashdi, S., Al-Sukaiti, N., Al-Adawi, K., Al-Riyami, M. and Al-Maawali, A. (2019) Biallelic mutations in AP3D1 cause Hermansky-Pudlak syndrome type 10 associated with immunodeficiency and seizure disorder. *Eur. J. Med. Genet.*, **62**, 103583.

62. Assoum, M., Philippe, C., Isidor, B., Perrin, L., Makrythanasis, P., Sondheimer, N., Paris, C., Douglas, J., Lesca, G., Antonarakis, S. *et al.* (2016) Autosomal-recessive mutations in AP3B2, adaptor-related protein complex 3 beta 2 subunit, cause an early-onset epileptic encephalopathy with optic atrophy. *Am. J. Hum. Genet.*, **99**, 1368–1376.

63. Abou Jamra, R., Philippe, O., Raas-Rothschild, A., Eck, S.H., Graf, E., Buchert, R., Borck, G., Ekici, A., Brockschmidt, F.F., Nothen, M.M. *et al.* (2011) Adaptor protein complex 4 deficiency causes severe autosomal-recessive intellectual disability, progressive spastic paraplegia, shy character, and short stature. *Am. J. Hum. Genet.*, **88**, 788–795.

64. Verkerk, A.J., Schot, R., Dumee, B., Schellekens, K., Swagemakers, S., Bertoli-Avella, A.M., Lequin, M.H., Dudink, J., Govaert, P., van Zwol, A.L. *et al.* (2009) Mutation in the AP4M1 gene provides a model for neuroaxonal injury in cerebral palsy. *Am. J. Hum. Genet.*, **85**, 40–52.

65. Morinaga, N., Tsai, S.C., Moss, J. and Vaughan, M. (1996) Isolation of a brefeldin A-inhibited guanine nucleotide-exchange protein for ADP ribosylation factor (ARF) 1 and ARF3 that contains a Sec7-like domain. *Proc. Natl. Acad. Sci. U. S. A.*, **93**, 12856–12860.

66. Hanai, A., Ohgi, M., Yagi, C., Ueda, T., Shin, H.W. and Nakayama, K. (2016) Class I Arfs (Arf1 and Arf3) and Arf6 are localized to the Flemming body and play important roles in cytokinesis. *J. Biochem.*, **159**, 201–208.

67. Pennauer, M., Buczak, K., Prescianotto-Baschong, C. and Spiess, M. (2022) Shared and specific functions of Arfs 1-5 at the Golgi revealed by systematic knockouts. *J. Cell Biol.*, **221**, e202106100.

68. Rasika, S., Passemard, S., Verloes, A., Gressens, P. and El Ghouzzi, V. (2018) Golgipathies in neurodevelopment: a new view of old defects. *Dev. Neurosci.*, **40**, 396–416.

69. Chardin, P. and McCormick, F. (1999) Brefeldin A: the advantage of being uncompetitive. *Cell*, **97**, 153–155.

70. Kikuchi, S., Shinpo, K., Tsuji, S., Yabe, I., Niino, M. and Tashiro, K. (2003) Brefeldin A-induced neurotoxicity in cultured spinal cord neurons. *J. Neurosci. Res.*, **71**, 591–599.

71. Paek, S.M. (2018) Recent synthesis and discovery of Brefeldin A analogs. *Mar. Drugs*, **16**, 133.

72. Rinaldi, C. and Wood, M.J.A. (2018) Antisense oligonucleotides: the next frontier for treatment of neurological disorders. *Nat. Rev. Neurol.*, **14**, 9–21.

73. Tanaka, A.J., Cho, M.T., Millan, F., Juusola, J., Retterer, K., Joshi, C., Niyazov, D., Garnica, A., Gratz, E., Deardorff, M. *et al.* (2015) Mutations in SPATA5 are associated with microcephaly, intellectual disability, seizures, and hearing loss. *Am. J. Hum. Genet.*, **97**, 457–464.

74. Cong, L., Ran, F.A., Cox, D., Lin, S., Barretto, R., Habib, N., Hsu, P.D., Wu, X., Jiang, W., Marraffini, L.A. and Zhang, F. (2013) Multiplex genome engineering using CRISPR/Cas systems. *Science*, **339**, 819–823.

75. Mattera, R., Arighi, C.N., Lodge, R., Zerial, M. and Bonifacino, J.S. (2003) Divalent interaction of the GGAs with the Rabaptin-5-Rabex-5 complex. *EMBO J.*, **22**, 78–88.

76. Lord, S.J., Velle, K.B., Mullins, R.D. and Fritz-Laylin, L.K. (2020) SuperPlots: communicating reproducibility and variability in cell biology. *J. Cell Biol.*, **219**, e202001064.